BRAIN CONNECTIVITY
Volume 1, Number 3, 2011

DOI: 10.1089/brain.2011.0032

Role of Ongoing, Intrinsic Activity of Neuronal Populations for Quantitative Neuroimaging of Functional Magnetic Resonance Imaging–Based Networks

Fahmeed Hyder,[1–4] Peter Herman,[1–3] Basavaraju G. Sanganahalli,[1–3] Daniel Coman,[1–3] Hal Blumenfeld,[2,5,6] and Douglas L. Rothman[1–4]

Abstract

A primary objective in neuroscience is to determine how neuronal populations process information within networks. In humans and animal models, functional magnetic resonance imaging (fMRI) is gaining increasing popularity for network mapping. Although neuroimaging with fMRI—conducted with or without tasks—is actively discovering new brain networks, current fMRI data analysis schemes disregard the importance of the total neuronal activity in a region. In task fMRI experiments, the baseline is differenced away to disclose areas of small evoked changes in the blood oxygenation level-dependent (BOLD) signal. In resting-state fMRI experiments, the spotlight is on regions revealed by correlations of tiny fluctuations in the baseline (or spontaneous) BOLD signal. Interpretation of fMRI-based networks is obscured further, because the BOLD signal indirectly reflects neuronal activity, and difference/correlation maps are thresholded. Since the small changes of BOLD signal typically observed in cognitive fMRI experiments represent a minimal fraction of the total energy/activity in a given area, the relevance of fMRI-based networks is uncertain, because the majority of neuronal energy/activity is ignored. Thus, another alternative for quantitative neuroimaging of fMRI-based networks is a perspective in which the activity of a neuronal population is accounted for by the demanded oxidative energy (CMR_{O2}). In this article, we argue that network mapping can be improved by including neuronal energy/activity of both the information about baseline and small differences/fluctuations of BOLD signal. Thus, total energy/activity information can be obtained through use of calibrated fMRI to quantify differences of ΔCMR_{O2} and through resting-state positron emission tomography/magnetic resonance spectroscopy measurements for average CMR_{O2}.

Key words: anesthesiology; brain metabolism; consciousness; magnetic resonance spectroscopic imaging (MRSI); positron emission tomography (PET)

Introduction

A principal goal in neuroscience is to understand how neuronal populations across different brain regions process information from the vibrant world, rich in moment-to-moment variations of sight, smell, sound, touch, and so on. A brain network, as discussed here, is defined as a subset of cortical and/or subcortical regions that functions (or works) together in an interconnected manner, either with a task (Friston, 1998) or when the brain is simply at rest (Biswal et al., 2010).

The mapping of brain networks in the awake, behaving human brain became possible about three decades ago with the application of positron emission tomography (PET) to measure blood flow and metabolic changes during cognitive and sensory stimuli. However, since that time, PET has largely been replaced by functional magnetic resonance imaging (fMRI), but the basic experimental paradigms and/or neuroimaging concepts have remained quite similar (Raichle, 2009). The main difference between neuroimaging with PET of old and fMRI of now is the fact that dynamic changes in blood oxygenation (i.e., combination of blood flow and

[1]Magnetic Resonance Research Center (MRRC), Yale University, New Haven, Connecticut.
[2]Core Center for Quantitative Neuroscience with Magnetic Resonance (QNMR), Yale University, New Haven, Connecticut.
Departments of [3]Diagnostic Radiology, [4]Biomedical Engineering, [5]Neurology, and [6]Neurobiology, Yale University, New Haven, Connecticut.

oxidative metabolism changes) can be repeatedly mapped in the same session.

The primary basis for localization of brain regions, whether isolated areas or network of areas, involved with cognitive or sensory paradigms is based on differences in regional brain activity between states (e.g., performing a task vs. performing a "different" task). However converging evidence shows that the neuronal activity represented in these difference maps is only a small fraction of the total neuronal activity in a region (Shulman, 1996; Shulman et al., 1999, 2001, 2009), particularly for cognitive tasks. Further, interpretation of fMRI-based networks with tasks becomes even more challenging, because the blood oxygenation level-dependent (BOLD) signal is an indirect measure of neuronal activity changes (Ogawa et al., 1993).

In this article, we review that the relationship between the brain's oxygen consumption and neuronal activity allows the fractional neuronal activity/energy involved in a difference map to be quantified relative to the resting-state (or baseline) activity/energy. In fact, it is shown that for both task-based fMRI (T-fMRI) and the newer resting-state fMRI (R-fMRI) paradigms, the changes in activity/energy being used to map networks represent a small fraction of the total activity/energy of any region involved. We propose as an alternative to measure the small differences/fluctuations of BOLD signal in relation to the total neuronal energy/activity in a given area. The total neuronal energy/activity can be measured by combining resting-state measurements of average energy consumption (e.g., by PET or magnetic resonance spectroscopy [MRS]) with the changes measured in calibrated fMRI studies, where the sum of these two measurements gives the total activity/energy in a region as a function of time. It is anticipated that future analysis of fMRI-based networks will include neuronal energy/activity of both the information about the baseline and small differences/fluctuations of BOLD signal for quantitative neuroimaging studies of brain networks (Hyder and Rothman, 2010, 2011).

Total Neuronal Activity Is Relevant for Studying Brain Networks

Traditionally, neural networks have been identified and distinguished according to their responses to sensory or cognitive stimuli. However, the brain detects stimuli reliably even when ambient (or background) conditions shift, due to external (e.g., light vs. dark) and/or internal (e.g., alert vs. sleepy) factors. Thus, recent investigations have incorporated independent measures of spontaneous activity as a means to evaluate the effect of the baseline on evoked responses. Experimental evidence strongly suggests that the total activity level reached on stimulation is quite independent of the baseline activity level (Hyder and Rothman, 2011).

Experiments using a variety of neuroimaging techniques (e.g., fMRI, optical imaging, electrophysiology), studying different sensory systems (e.g., somatosensory cortex, visual cortex, and olfactory bulb), across a range of species (e.g., rat, cat, monkey, human), and under diverse experimental conditions (e.g., awake, sleep, and anesthetized) show that the total neuronal activity reached on stimulation is, to a first order, independent of the spontaneous (i.e., nonevoked) baseline state neuronal activity (Chen et al., 2005; Issa and Wang, 2008, 2009; Li et al., 2011; Maandag et al., 2007; Masamoto et al., 2007; Pasley et al., 2007; Portas et al., 2000; Smith et al., 2002; Uludag et al., 2004; Zhu et al., 2009b). These results, in general, imply that there may be inherent neuronal mechanisms to ensure a similar level of information transfer from sensory input, regardless of external or internal situations that may impact the brain's baseline state. Most importantly, these findings emphasize the need to understand the role of baseline activity of neuronal populations within the context of networks (Hyder and Rothman, 2010).

Total Brain Activity Is Much Higher than Differences or Fluctuations Measured in fMRI studies

In T-fMRI experiments, traditionally subtracting the baseline signal was justified by an assumption that there was very little baseline neuronal activity (and by inference, demanded energy) in the awake state (Posner and Raichle, 1998). However, resting-state measurements—including MRS (^{13}C, ^{31}P, ^{17}O) and PET—have shown this hypothesis to be incorrect (Alkire, 2008; Boumezbeur et al., 2010; Du et al., 2008; Zhu et al., 2009b). In the awake human brain, in fact, the total neuronal activity (or energy) in the resting state is much higher than the activity (or energy) evoked by cognitive stimuli (Shulman et al., 2009). As described next, the subtraction-based method may lead to very different interpretation when resting-state neuronal activity is subtracted from the activity during stimulation.

Several methods now exist to measure total brain neuronal activity (or energy). Tissue oxygen tension (pO_2) can be used to infer local dynamics of uncoupling between oxygen delivery (i.e., combining blood flow [CBF]) and its subsequent utilization (i.e., oxidative energy demand [CMR_{O2}]) (Ances et al., 2001), but its invasiveness limits translation to humans. On the other hand, PET measures CMR_{O2} noninvasively, but requires use of multiple radioactive tracers (Ito et al., 2005). MRS utilizing detection of nonradioactive ^{17}O isotope can also measure CMR_{O2} noninvasively (Zhu et al., 2005), whereas ^{13}C MRS used in conjunction with different ^{13}C-labeled substrates (e.g., glucose or acetate) can distinguish between energetic demands of neurons and astrocytes (Hyder et al., 2006). Both these MRS techniques, however, have lower spatial resolution compared with MRI and PET. Although the PET and MRS methods (for resting-state CMR_{O2}) suffer from lower temporal and spatial resolution than fMRI, as described next in conjunction with quantitative calibrated fMRI measurements (for ΔCMR_{O2} with task), together they can provide a map of total brain activity in the paradigms presently used to map networks by fMRI. Since recent advances in ^{17}O MRS allow whole brain mapping of CMR_{O2} in awake, behaving humans (Atkinson and Thulborn, 2010), it may be possible to combine future network studies with calibrated fMRI for ΔCMR_{O2} with task in conjunction with ^{17}O MRS for resting-state CMR_{O2} (Zhu et al., 2009b).

Challenges in Utilizing Activation and Correlation Maps for Brain Connectivities

The BOLD signal is sensitive to concentrations of oxyhemoglobin (diamagnetic) versus deoxyhemoglobin (paramagnetic), and the contrast is positive (i.e., $\Delta S/S > 0$ in Eq. 1; see below) when deoxyhemoglobin is reduced in the microvasculature (Ogawa et al., 1990) to deliver more oxygen from the blood in support of increased functional energy demand (Hyder et al., 1998). As demonstrated from the earliest days

of fMRI in 1992, change in the BOLD signal is usually quite small (Bandettini et al., 1992; Blamire et al., 1992; Frahm et al., 1992; Kwong et al., 1992; Ogawa et al., 1992). However, the BOLD contrast is usually interpreted from an unspecified baseline state, and moreover, there is no true baseline, because the brain is never actually at rest (Shulman and Rothman, 1998; Shulman et al., 2007)—measured either in terms of neuronal activity (Arieli et al., 1996) or the energy that these activities demand (Smith et al., 2002).

Neuroscientists originally used fMRI with task-based paradigms (or T-fMRI), in which the mean of the baseline state is subtracted from the mean of the stimulated state, to unveil activated (or deactivated) regions associated with the task (Huettel et al., 2004). T-fMRI experiments in the human brain generally report small evoked changes in the BOLD signal that peaks within ~ 6 sec after task onset. The magnitude of the evoked BOLD response varies with the task type (e.g., sensory and cognitive) and with the cortical area (i.e., $>1\%$ and $<1\%$, respectively, in primary sensory and high-order areas). Many brain networks have been reported for a wide range of cognitive modules with T-fMRI data (Frackowiak et al., 2004; Huettel et al., 2004).

However, fMRI is also used to study the brain at rest in the absence of any explicit tasks. Biswal and associates (1995) observed that resting human brain fMRI data contain small-amplitude ($\sim 1\%$), low-frequency (<0.1 Hz) fluctuations in the spontaneous BOLD signal that are temporally correlated across vast spans of cerebral cortex. Although in the R-fMRI paradigm, the baseline signal is not exactly differenced away, it is exclusively the deviations of the BOLD signal that are used to create spatiotemporal coherence maps to represent correlated networks (Fox et al., 2005). Today, R-fMRI is the primary method by which brain networks are generated for cognitive modules (Tomasi and Volkow, 2011; van den Heuvel and Hulshoff Pol, 2010)

Data analysis in cognitive fMRI studies, however, are based on very small evoked (i.e., T-fMRI) and spontaneous (i.e., R-fMRI) changes in the BOLD signal. For T-fMRI experiments, results from sensory paradigms show slightly better reproducibility than results from cognitive paradigms primarily because of marginally higher magnitude BOLD response observed with sensory versus cognitive stimuli (Lund et al., 2005; McGonigle et al., 2000). For R-fMRI experiments, however, reproducibility is rarely assessed, because long duration scans are used to create the correlation maps where repeated runs are quite uncommon, and/or the status quo is the group-averaged data of networks (Habeck and Moeller, 2011). Since these activation and correlation maps—generated, respectively, from T-fMRI and R-fMRI data—likely possess large inter-session and/or inter-subject variability (Biswal et al., 2010; Wei et al., 2004), cognitive fMRI studies use conjunction analysis (Friston et al., 1999; Shulman et al., 1997).

The conjunction analysis scheme uses all subjects' maps in order to co-localize where each subject activated (or deactivated) and show correlations (positive or negative). The end result is the appearance of "large" brain networks that span across the cerebral cortex (Fox et al., 2005; Shulman et al., 1997). However, it is also quite possible that this procedure masks experimental variability which arises due to baseline variations across studies, either in different sessions and/or across subjects. Since the baseline signal is relevant for fMRI-based networks, future studies with superior BOLD contrast at higher magnetic fields should seek to resolve the sensitivity/reproducibility issue for both T-fMRI and R-fMRI so that conjunction analysis is not a necessity for data processing (Feinberg et al., 2010; Poser et al., 2010).

Although T-fMRI was the primary way in which brain networks were created up until the early part of this decade (Friston, 1998), R-fMRI is now the status quo approach to generate networks for a wide range of cognitive modules (Raichle, 2010). R-fMRI data are analyzed for spatiotemporal coherence to reveal correlated networks. A pre-processing step is to regress out contributions from the global BOLD signal fluctuations (Macey et al., 2004; Fox et al., 2005). This process presumably eliminates "physiological noise" from nonneuronal sources (Birn et al., 2006; Chang and Glover, 2009) and/or uncorrelated neuronal activities. The remaining smaller (or filtered) fluctuations in the spontaneous BOLD signal facilitate detection of network-level correlations (Fox et al., 2005; Greicius et al., 2003). These tiny fluctuations in the spontaneous BOLD signal are often assigned to neuronal activity that supports networks (e.g., the default mode) and are believed to be representative of some aspect of resting brain function rather than the total neuronal activity characterizing the baseline state (Shulman et al., 2007). If, however, there is a significant correlated neuronal component associated with the global BOLD signal, then important information about resting-state brain connectivity could be discarded by this process (Scholvinck et al., 2010).

Recently, Schölvinck and associates (2010) demonstrated that the global component of BOLD signal fluctuations measured at rest is indeed tightly coupled with a slow modulation of neuronal events which appear to be ubiquitous in the cerebral cortex. They thereby recommend caution when arbitrarily removing the global BOLD signal, because in doing so, a global correlate of the brain's baseline neuronal activity is thrown away and, which, in turn, may also affect regions that are defined as either correlated or anti-correlated. Thus, the Schölvinck and associates study has strong ramifications for interpretation of default mode or other networks using R-fMRI data that are assigned based on removal of the global average fluctuations of the BOLD signal.

Although correlations between slow (<0.1 Hz) modulations of ongoing neuronal activity, as measured by local field potential (LFP) and/or multi-unit activity (MUA), and fluctuations of the resting BOLD signal have been previously reported both locally near the microelectrode and extending over regions of the visual cortex (Shmuel and Leopold, 2008), the study by Schölvinck and associates show that these correlations extend over nearly the entire cortical surface with a correlation strength that is not obviously related to the position of the electrode. They simultaneously recorded LFP and BOLD signal from the resting, awake primate brain and compared a regional fMRI signal with the slow temporal variations in the power of the LFP in low, intermediate, and high-frequency bands (see (Buzsaki and Draguhn, 2004) for frequency distributions of neuronal activities). Slow fluctuations of the spontaneous neuronal activity—in either high or low, but not intermediate, frequency LFP bands—measured from a single cortical site in one hemisphere exhibited widespread correlations with spontaneous fluctuations in BOLD signals. Global patterns of these (positive) spatial correlations were quite similar

whether the LFP was measured from the frontal, parietal, or occipital cortices.

The disadvantage of cross-correlation-based connectivity analysis of R-fMRI data is that it requires a priori knowledge or a hypothesis about inherent spatial connectivity. Since the cross-correlation method assumes a seed region and assesses the functional connectivity of that region with other areas, future R-fMRI data analysis should consider nonseeded approaches such as independent component analysis and fractal analysis (Herman et al., 2011; Hutchison et al., 2010). Independent component analysis was developed for linear representation of mixed data (Bell and Sejnowski, 1995), with the aim of identifying non-gaussian independent components that underlie unique neural networks. Since the number of independent components are usually larger than the number of expected neural networks (Calhoun et al., 2001), the signals giving rise to the independent components are transformed to a z-score, thresholded, and associated with known anatomical or functional systems by visual inspection, whereas the unidentified components are discarded.

Both cross-correlation analysis and independent component analysis, however, simultaneously use all BOLD signal time series (i.e., from all voxels) to get a single, final parameter to describe the connectivity. In contrast, fractal analysis, which is a scale-free examination of fluctuating data (Mandelbrot and van Ness, 1968), calculates a fractal parameter independently for each BOLD signal time series (i.e., from each voxel). Thus, a fractal parameter map itself can be used to define subtle changes across brain states (Wang et al., 2011) and/or regional variations (Herman et al., 2011). Since the fractal parameter captures the unique behavior of the fluctuating signal that is governed by physiological processes (see Eke et al., 2002 for details on fractal analysis), it could potentially be used for network identification without experimental bias of visual inspection.

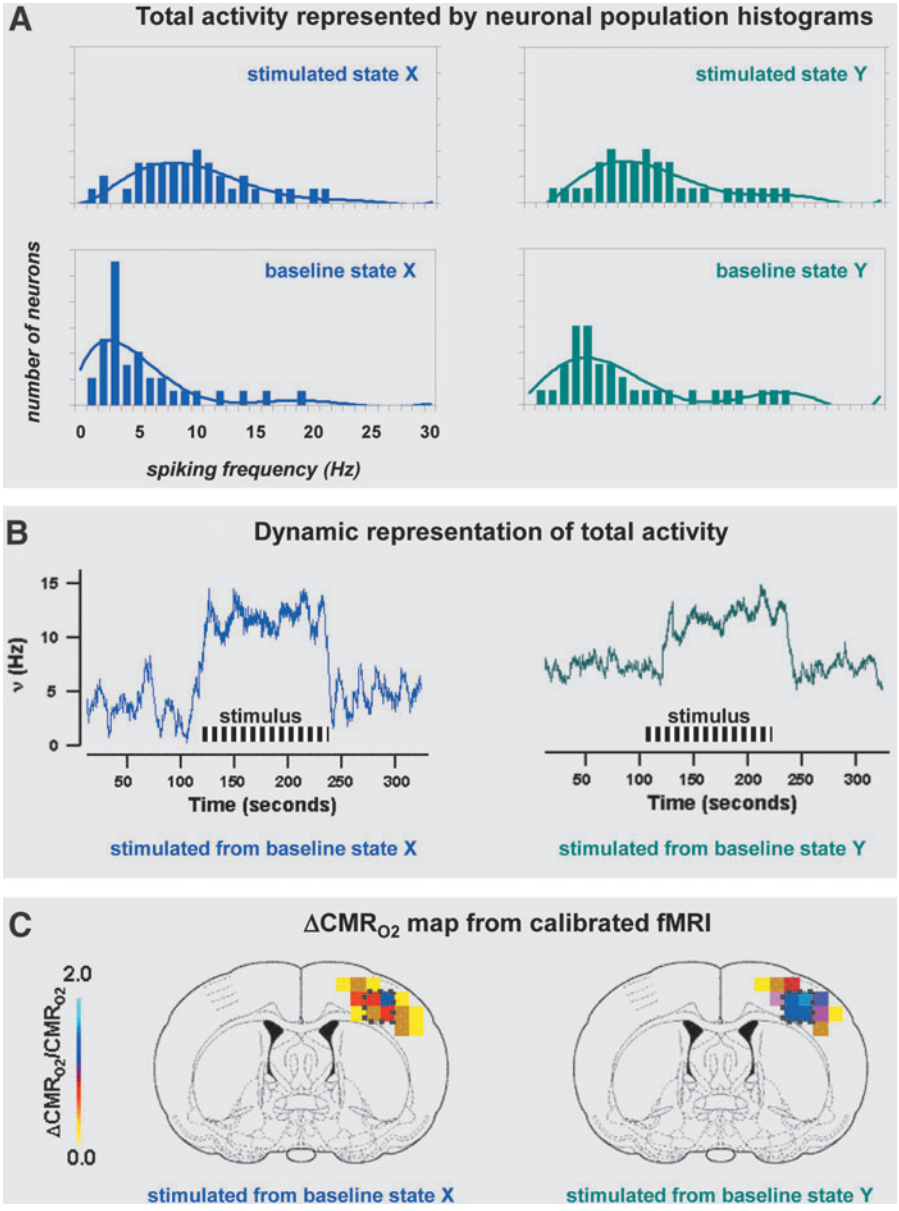

FIG. 1. **(A)** Total activity represented by neuronal population histograms. Neuronal activity for baseline and stimulated states, X and Y, represented in terms of neuronal population histograms (i.e., number of neurons firing at given spike rate). The stimulated states X and Y show very similar distributions, whereas the baseline states X and Y show very different distributions. The baseline state X is lower than baseline state Y when Eq. A1 (see Appendix) is applied to estimate (relative) baseline CMR_{O2} values for each state. **(B)** Dynamic representation of total activity. *In vivo* time courses of the spiking rate of a neuronal ensemble *in vivo* for baseline states X and Y (from the same rat) during sensory stimulation. The total activity reached on stimulation for both states is quite similar as suggested from the neuronal histograms. The evoked change in neuronal activity with stimulation is much larger from baseline state X. **(C)** ΔCMR_{O2} map from calibrated fMRI. *In vivo* averaged ΔCMR_{O2} maps for baseline states X and Y (from the same rat) during sensory stimulation. The evoked change in CMR_{O2} with stimulation is much larger from baseline state X. All data from (Smith et al., 2002). See Appendix for a detailed explanation. CMR_{O2}, oxidative energy demand; fMRI, functional magnetic resonance imaging.

Mapping Neuronal Activity with Calibrated fMRI and Related Techniques

Since activation maps (from T-fMRI data) and correlation maps (from R-fMRI data) are actually statistical parametric maps generated from weak BOLD contrasts (Frackowiak et al., 2004; Huettel et al., 2004), these threshold-based maps are not necessarily directly proportional to changes in neuronal activity. Moreover, the few select regions that survive statistical significance are revealed by using rather arbitrary thresholds (van Eijsden et al., 2009).

Thus, recently, there has been renewed interest in mapping oxidative energy (CMR_{O2}) as a close approximation for neuronal activity (Hyder et al., 2002). The interest in CMR_{O2} is because studies using MRS and other modalities show that there is a direct relationship in the brain between neuronal activity, as measured by electrical activity or neurotransmitter release and recycling, and the amount of oxygen the neurons consume (Hyder et al., 2006).

With calibrated fMRI, it is feasible to calculate ΔCMR_{O2} from changes in the BOLD signal (S) along with CBF and/or volume (CBV) measurements (Davis et al., 1998) according to the relationship

$$\frac{\Delta CMR_{O2}}{CMR_{O2}} = \frac{\Delta CBF}{CBF} - \left(\frac{1}{A}\frac{\Delta S}{S} + \frac{\Delta CBV}{CBV}\right)\left(1 + \frac{\Delta CBF}{CBF}\right) \quad (1)$$

where A in Eq. 1 is a measurable physiologic constant (Hyder et al., 2001). The basis for ΔCMR_{O2} mapping, either with or without tasks, using calibrated fMRI is that it reflects the oxidative ATP demanded for neuronal work (Hoge and Pike, 2001). Thus, Eq. 1 can be described with both neurovascular and neurometabolic couplings (Hyder et al., 2010): "neurovascular coupling" relates local changes in neuronal activity and constriction/dilation of blood vessels to decrease/increase CBF and/or CBV to a region, whereas "neurometabolic coupling" relates focal alterations in neuronal activity to CMR_{O2} to keep pace with cellular ATP demand.

Recent calibrated fMRI studies in rats report that magnitudes of ΔCMR_{O2} during sensory stimulation—conducted at magnetic fields of 7T and higher—are commensurate with changes in neuronal firing under steady-state conditions (Kida et al., 2006; Maandag et al., 2007; Smith et al., 2002). Neural activity, measured by extracellular recordings, can be quantified in terms of spiking rate (or frequency) of many neurons (Smith et al., 2002; Maandag et al., 2007). A descriptive example from Smith and associates illustrates behavior of the same neuronal population (Fig. 1A) as well as its dynamic pattern (Fig. 1B) when stimulated with the same stimulus, but from different baselines states. On stimulation, the neuronal activities reach the same levels (Fig. 1B) and these agree well with magnitudes of ΔCMR_{O2} (from calibrated fMRI) during sensory stimulation (Fig. 1C).

More recent rat calibrated fMRI studies have elucidated the dynamic relationships between CBF, CBV, and BOLD signals in relation to the underlying neurophysiology to determine transient CMR_{O2} changes with dynamic calibrated fMRI (Herman et al., 2009; Hyder et al., 2010; Kida et al., 2007; Sanganahalli et al., 2009). CMR_{O2} changes, steady state or transient, derived from calibrated fMRI compare well with neuronal activity recordings of LFP and/or MUA during sensory stimulation.

A key observation is that although relationships between neuronal activity and sensory stimulus features range from linear to nonlinear, associations between neuroimaging signals (BOLD, CBF, and CBV) and neuronal activity (LFP, MUA) are almost always linear (Fig. 2A). Most importantly, the results demonstrate good agreement between the changes in CMR_{O2} and independent measures of LFP or MUA (Fig. 2B). A consequence of the tight neurovascular and neurometabolic couplings observed from steady-state conditions to

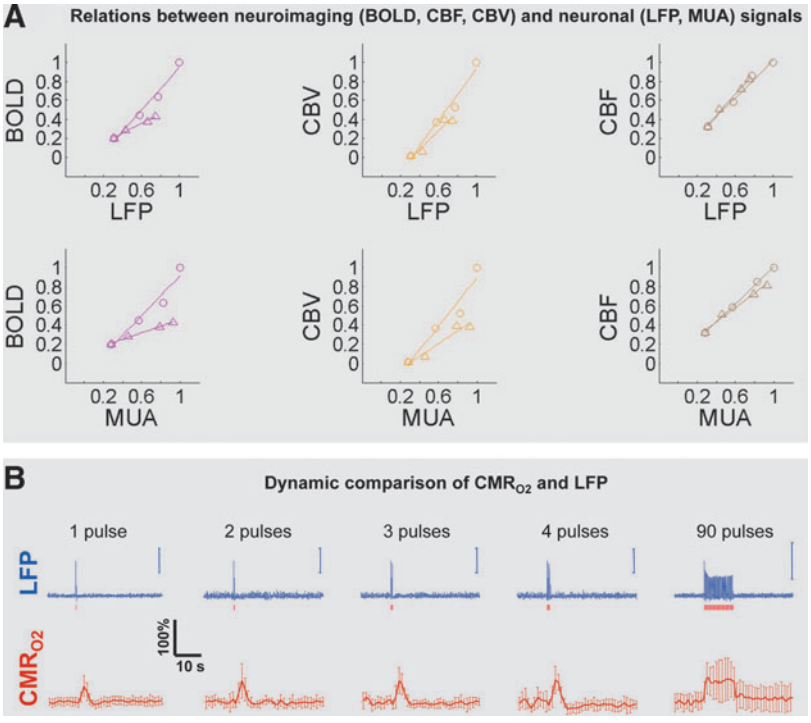

FIG. 2. **(A)** Relations between neuroimaging signals (BOLD, CBF, and CBV) and neuronal activity (LFP, MUA). Evoked neuronal activity (LFP and MUA) show linear correlations with evoked neuroimaging signals (BOLD, CBF, and CBV) with increasing number of stimulus pulses at rates of 1.5 Hz (○) and 3 Hz (Δ). The multi-modal data suggest tight neurovascular coupling. **(B)** Dynamic comparison of ΔCMR_{O2} and LFP (for 3 Hz stimulation frequency). The dynamic correlation between the calculated ΔCMR_{O2} and the measured LFP suggests tight neurometabolic coupling. All data from (Herman et al., 2009) and (Sanganahalli et al., 2009). BOLD, blood oxygenation level-dependent; CBF, cerebral blood flow; CBV, cerebral blood volume; LFP, local field potential; MUA, multi-unit activity.

events separated by <200 msec is that there is very rapid oxygen equilibration between blood and tissue pools (Herman et al., 2006; Vazquez et al., 2008).

Although these calibrated fMRI studies emphasize quantifying ΔCMR_{O2} for evoked BOLD signal during stimulation, estimates for ΔCMR_{O2} for spontaneous BOLD signal (i.e., at rest) can be made from just the fluctuations, either before or after the stimulus, for example, see Figure 2B. We estimate a maximum ΔCMR_{O2} of 10% for spontaneous fluctuations of the BOLD signal from the rat calibrated fMRI results. It is noted that less than 10% change in CMR_{O2} is generally observed with cognitive tasks in awake, behaving humans (Rothman et al., 2002; Shulman et al., 2001).

For future brain network studies, we propose to measure small differences/fluctuations of CMR_{O2} by calibrated fMRI and the baseline information on CMR_{O2} by ^{17}O MRS (Zhu et al., 2009b). Since there are regional variations in energy metabolism in the awake human brain both at rest and during cognition (Horwitz et al., 1984; Roland et al., 1987), using both ΔCMR_{O2} and CMR_{O2} information in brain connectivities should be considered.

Conclusions

Since many vital functions (e.g., foraging, mating, survival, etc.) depend on the brain's ability to perceive the dynamically varying environment, neuronal systems need to accurately detect and process external stimuli under widely different operational circumstances (Hyder et al., 2002). Indeed, an echoing principle in many studies (Chen et al., 2005; Issa and Wang, 2008, 2009; Li et al., 2011; Maandag et al., 2007; Masamoto et al., 2007; Pasley et al., 2007; Portas et al., 2000; Smith et al., 2002; Uludag et al., 2004; Zhu et al., 2009b) is that the total neuronal activity in any given state is relevant for understanding brain function, from rest to stimulation (Hyder and Rothman, 2010; Northoff et al., 2010).

At present, R-fMRI and T-fMRI studies discard the global baseline activity and the global component of spontaneous fluctuations of the BOLD signal. The global baseline neuronal activity and its requisite energy demand is extremely high for the cerebral cortex of the awake human (Shulman et al., 2009), and as just discussed, the spontaneous fluctuations may be in the order of changes generally observed in cognitive tasks. In light of these findings, therefore, the measurement of the total neural activity can add an important factor for the consideration of reliability for the estimated neural networks.

Acknowledgment

The authors thank their colleagues at Yale for their insightful comments. This work was supported by National Institutes of Health Grants (R01 MH-067528 to F.H., P30 NS-052519 to F.H., R01 NS-049307 to H.B., R01 NS-066974 to H.B., and R01 AG-034953 to D.L.R.).

Author Disclosure Statement

No competing financial interests exist.

References

Alkire MT. 2008. Loss of effective connectivity during general anesthesia. Int Anesthesiol Clin 46:55–73.

Ances BM, Buerk DG, Greenberg JH, Detre JA. 2001. Temporal dynamics of the partial pressure of brain tissue oxygen during functional forepaw stimulation in rats. Neurosci Lett 306: 106–110.

Arieli A, Sterkin A, Grinvald A, Aertsen A. 1996. Dynamics of ongoing activity: explanation of the large variability in evoked cortical responses. Science 273:1868–1871.

Atkinson IC, Thulborn KR. 2010. Feasibility of mapping the tissue mass corrected bioscale of cerebral metabolic rate of oxygen consumption using 17-oxygen and 23-sodium MR imaging in a human brain at 9.4 T. Neuroimage 51: 723–733.

Bandettini PA, Wong EC, Hinks RS, Tikofsky RS, Hyde JS. 1992. Time course EPI of human brain function during task activation. Magn Reson Med 25:390–397.

Bell AJ, Sejnowski TJ. 1995. An information-maximization approach to blind separation and blind deconvolution. Neural Comput 7:1129–1159.

Birn RM, Diamond JB, Smith MA, Bandettini PA. 2006. Separating respiratory-variation-related fluctuations from neuronal-activity-related fluctuations in fMRI. Neuroimage 31: 1536–1548.

Biswal B, Yetkin FZ, Haughton VM, Hyde JS. 1995. Functional connectivity in the motor cortex of resting human brain using echo-planar MRI. Magn Reson Med 34:537–541.

Biswal BB, Mennes M, Zuo XN, Gohel S, Kelly C, Smith SM, Beckmann CF, Adelstein JS, Buckner RL, Colcombe S, Dogonowski AM, Ernst M, Fair D, Hampson M, Hoptman MJ, Hyde JS, Kiviniemi VJ, Kotter R, Li SJ, Lin CP, Lowe MJ, Mackay C, Madden DJ, Madsen KH, Margulies DS, Mayberg HS, McMahon K, Monk CS, Mostofsky SH, Nagel BJ, Pekar JJ, Peltier SJ, Petersen SE, Riedl V, Rombouts SA, Rypma B, Schlaggar BL, Schmidt S, Seidler RD, Siegle GJ, Sorg C, Teng GJ, Veijola J, Villringer A, Walter M, Wang L, Weng XC, Whitfield-Gabrieli S, Williamson P, Windischberger C, Zang YF, Zhang HY, Castellanos FX, Milham MP. 2010. Toward discovery science of human brain function. Proc Natl Acad Sci U S A 107:4734–4739.

Blamire AM, Ogawa S, Ugurbil K, Rothman D, McCarthy G, Ellermann JM, Hyder F, Rattner Z, Shulman RG. 1992. Dynamic mapping of the human visual cortex by high-speed magnetic resonance imaging. Proc Natl Acad Sci U S A 89:11069–11073.

Boumezbeur F, Mason GF, de Graaf RA, Behar KL, Cline GW, Shulman GI, Rothman DL, Petersen KF. 2010. Altered brain mitochondrial metabolism in healthy aging as assessed by in vivo magnetic resonance spectroscopy. J Cereb Blood Flow Metab 30:211–221.

Buzsaki G, Draguhn A. 2004. Neuronal oscillations in cortical networks. Science 304:1926–1929.

Calhoun VD, Adali T, McGinty VB, Pekar JJ, Watson TD, Pearlson GD. 2001. fMRI activation in a visual-perception task: network of areas detected using the general linear model and independent components analysis. Neuroimage 14:1080–1088.

Chang C, Glover GH. 2009. Effects of model-based physiological noise correction on default mode network anti-correlations and correlations. Neuroimage 47:1448–1459.

Chen LM, Friedman RM, Roe AW. 2005. Optical imaging of SI topography in anesthetized and awake squirrel monkeys. J Neurosci 25:7648–7659.

Davis TL, Kwong KK, Weisskoff RM, Rosen BR. 1998. Calibrated functional MRI: mapping the dynamics of oxidative metabolism. Proc Natl Acad Sci U S A 95:1834–1839.

Du F, Zhu XH, Zhang Y, Friedman M, Zhang N, Ugurbil K, Chen W. 2008. Tightly coupled brain activity and cerebral ATP metabolic rate. Proc Natl Acad Sci U S A 105:6409–6414.

Eke A, Herman P, Kocsis L, Kozak LR. 2002. Fractal characterization of complexity in temporal physiological signals. Physiol Meas 23:R1–R38.

Feinberg DA, Moeller S, Smith SM, Auerbach E, Ramanna S, Glasser MF, Miller KL, Ugurbil K, Yacoub E. 2010. Multiplexed echo planar imaging for sub-second whole brain FMRI and fast diffusion imaging. PLoS One 5:e15710.

Fox MD, Snyder AZ, Vincent JL, Corbetta M, Van Essen DC, Raichle ME. 2005. The human brain is intrinsically organized into dynamic, anticorrelated functional networks. Proc Natl Acad Sci U S A 102:9673–9678.

Frackowiak RSJ, Ashburner JT, Penny WD, Zeki S, Friston KJ, Frith CD, Dolan RJ, Price CJ. 2004. *Human Brain Function*. San Diego, CA: Elsevier Academic Press.

Frahm J, Bruhn H, Merboldt KD, Hanicke W. 1992. Dynamic MR imaging of human brain oxygenation during rest and photic stimulation. J Magn Reson Imaging 2:501–505.

Friston KJ. 1998. Imaging neuroscience: principles or maps? Proc Natl Acad Sci U S A 95:796–802.

Friston KJ, Holmes AP, Price CJ, Buchel C, Worsley KJ. 1999. Multisubject fMRI studies and conjunction analyses. Neuroimage 10:385–396.

Greicius MD, Krasnow B, Reiss AL, Menon V. 2003. Functional connectivity in the resting brain: a network analysis of the default mode hypothesis. Proc Natl Acad Sci U S A 100:253–258.

Habeck C, Moeller JR. 2011. Intrinsic functional-connectivity networks for diagnosis: just beautiful pictures? Brain Connectivity 1:99–103.

Herman P, Sanganahalli BG, Blumenfeld H, Hyder F. 2009. Cerebral oxygen demand for short-lived and steady-state events. J Neurochem 109 Suppl 1:73–79.

Herman P, Sanganahalli BG, Hyder F, Eke A. 2011. Fractal analysis of spontaneous fluctuations of the BOLD signal in rat brain. Neuroimage. DOI. 10.1016/j.neuroimage.2011.06.082 [Epub ahead of print].

Herman P, Trubel HK, Hyder F. 2006. A multiparametric assessment of oxygen efflux from the brain. J Cereb Blood Flow Metab 26:79–91.

Hoge RD, Pike GB. 2001. Oxidative metabolism and the detection of neuronal activation via imaging. J Chem Neuroanat. 22:43–52.

Horwitz B, Duara R, Rapoport SI. 1984. Intercorrelations of glucose metabolic rates between brain regions: application to healthy males in a state of reduced sensory input. J Cereb Blood Flow Metab. 4:484–499.

Huettel SA, Song AW, McCarthy G. 2004. *Functional Magnetic Resonance Imaging*. Sunderland, MA: Sinauer.

Hutchison RM, Mirsattari SM, Jones CK, Gati JS, Leung LS. 2010. Functional networks in the anesthetized rat brain revealed by independent component analysis of resting-state FMRI. J Neurophysiol 103:3398–3406.

Hyder F, Kida I, Behar KL, Kennan RP, Maciejewski PK, Rothman DL. 2001. Quantitative functional imaging of the brain: towards mapping neuronal activity by BOLD fMRI. NMR Biomed 14:413–431.

Hyder F, Patel AB, Gjedde A, Rothman DL, Behar KL, Shulman RG. 2006. Neuronal-glial glucose oxidation and glutamatergic-GABAergic function. J Cereb Blood Flow Metab 26:865–877.

Hyder F, Rothman DL. 2010. Neuronal correlate of BOLD signal fluctuations at rest: err on the side of the baseline. Proc Natl Acad Sci U S A 107:10773–10774.

Hyder F, Rothman DL. 2011. Evidence for the importance of measuring total brain activity in neuroimaging. Proc Natl Acad Sci U S A 108:5475–5476.

Hyder F, Rothman DL, Shulman RG. 2002. Total neuroenergetics support localized brain activity: implications for the interpretation of fMRI. Proc Natl Acad Sci U S A 99:10771–10776.

Hyder F, Sanganahalli BG, Herman P, Coman D, Maandag NJ, Behar KL, Blumenfeld H, Rothman DL. 2010. Neurovascular and neurometabolic couplings in dynamic calibrated fMRI: transient oxidative neuroenergetics for block-design and event-related paradigms. Front Neuroenergetics 2:pii, 18.

Hyder F, Shulman RG, Rothman DL. 1998. A model for the regulation of cerebral oxygen delivery. J Appl Physiol 85:554–564.

Issa EB, Wang X. 2008. Sensory responses during sleep in primate primary and secondary auditory cortex. J Neurosci 28:14467–14480.

Issa EB, Wang X. 2009. Altered neural responses to sounds in primate primary auditory cortex during slow-wave sleep. J Neurosci 31:2965–2973.

Ito H, Kanno I, Fukuda H. 2005. Human cerebral circulation: positron emission tomography studies. Ann Nucl Med 19:65–74.

Kida I, Rothman DL, Hyder F. 2007. Dynamics of changes in blood flow, volume, and oxygenation: implications for dynamic functional magnetic resonance imaging calibration. J Cereb Blood Flow Metab 27:690–696.

Kida I, Smith AJ, Blumenfeld H, Behar KL, Hyder F. 2006. Lamotrigine suppresses neurophysiological responses to somatosensory stimulation in the rodent. Neuroimage 29:216–224.

Kwong KK, Belliveau JW, Chesler DA, Goldberg IE, Weisskoff RM, Poncelet BP, Kennedy DN, Hoppel BE, Cohen MS, Turner R, et al. 1992. Dynamic magnetic resonance imaging of human brain activity during primary sensory stimulation. Proc Natl Acad Sci U S A 89:5675–5679.

Li A, Gong L, Xu F. 2011. Brain-state-independent neural representation of peripheral stimulation in rat olfactory bulb. Proc Natl Acad Sci U S A 108:5087–5092.

Lund TE, Norgaard MD, Rostrup E, Rowe JB, Paulson OB. 2005. Motion or activity: their role in intra- and inter-subject variation in fMRI. Neuroimage 26:960–964.

Maandag NJ, Coman D, Sanganahalli BG, Herman P, Smith AJ, Blumenfeld H, Shulman RG, Hyder F. 2007. Energetics of neuronal signaling and fMRI activity. Proc Natl Acad Sci U S A 104:20546–20551.

Macey PM, Macey KE, Kumar R, Harper RM. 2004. A method for removal of global effects from fMRI time series. Neuroimage 22:360–366.

Mandelbrot B, van Ness J. 1968. Fractional brownian motions, fractional noises and applications. SIAM Rev 10:422–437.

Masamoto K, Kim T, Fukuda M, Wang P, Kim SG. 2007. Relationship between neural, vascular, and BOLD signals in isoflurane-anesthetized rat somatosensory cortex. Cereb Cortex 17:942–950.

McGonigle DJ, Howseman AM, Athwal BS, Friston KJ, Frackowiak RS, Holmes AP. 2000. Variability in fMRI: an examination of intersession differences. Neuroimage 11:708–734.

Northoff G, Duncan NW, Hayes DJ. 2010. The brain and its resting state activity—experimental and methodological implications. Prog Neurobiol 92:593–600.

Ogawa S, Lee TM, Kay AR, Tank DW. 1990. Brain magnetic resonance imaging with contrast dependent on blood oxygenation. Proc Natl Acad Sci U S A 87:9868–9872.

Ogawa S, Menon RS, Tank DW, Kim SG, Merkle H, Ellermann JM, Ugurbil K. 1993. Functional brain mapping by blood

oxygenation level-dependent contrast magnetic resonance imaging. A comparison of signal characteristics with a biophysical model. Biophys J 64:803–812.
Ogawa S, Tank DW, Menon R, Ellermann JM, Kim SG, Merkle H, Ugurbil K. 1992. Intrinsic signal changes accompanying sensory stimulation: functional brain mapping with magnetic resonance imaging. Proc Natl Acad Sci U S A 89:5951–5955.
Pasley BN, Inglis BA, Freeman RD. 2007. Analysis of oxygen metabolism implies a neural origin for the negative BOLD response in human visual cortex. Neuroimage 36:269–276.
Portas CM, Krakow K, Allen P, Josephs O, Armony JL, Frith CD. 2000. Auditory processing across the sleep-wake cycle: simultaneous EEG and fMRI monitoring in humans. Neuron 28:991–999.
Poser BA, Koopmans PJ, Witzel T, Wald LL, Barth M. 2010. Three dimensional echo-planar imaging at 7 Tesla. Neuroimage 51:261–266.
Posner MI, Raichle ME. 1998. The neuroimaging of human brain function. Proc Natl Acad Sci U S A 95:763–764.
Raichle ME. 2009. A brief history of human brain mapping. Trends Neurosci 32:118–126.
Raichle ME. 2010. Two views of brain function. Trends Cogn Sci 14:180–190.
Roland PE, Eriksson L, Stone-Elander S, Widen L. 1987. Does mental activity change the oxidative metabolism of the brain? J Neurosci 7:2373–2389.
Rothman DL, Hyder F, Sibson NR, Behar KL, Mason GF, Shen J, Petroff OAC, Shulman RG. 2002. In vivo magnetic resonance spectroscopy studies of the glutamate and GABA neurotransmitter cycles and functional neuroenergetics. In: Davis KL, Charney D, Coyle JT, Nemeroff C (eds.). *Neuropsychopharmacology: The Fifth Generation of Progress.* Philadelphia, PA: Lippincott Williams & Wilkins; pp. 315–342.
Sanganahalli BG, Herman P, Blumenfeld H, Hyder F. 2009. Oxidative neuroenergetics in event-related paradigms. J Neurosci 29:1707–1718.
Scholvinck ML, Maier A, Ye FQ, Duyn JH, Leopold DA. 2010. Neural basis of global resting-state fMRI activity. Proc Natl Acad Sci U S A 107:10238–10243.
Shmuel A, Leopold DA. 2008. Neuronal correlates of spontaneous fluctuations in fMRI signals in monkey visual cortex: implications for functional connectivity at rest. Hum Brain Mapp 29:751–761.
Shulman GI, Fiez JA, Corbetta M, Buckner RL, Miezin FM, Raichle ME, Petersen SE. 1997. Common Blood Flow Changes across Visual Tasks: II. Decreases in Cerebral Cortex. J Cogn Neurosci 9:648–663.
Shulman RG. 1996. Interview with Robert G. Shulman. J Cogn Neurosci 8:474–480.
Shulman RG, Hyder F, Rothman DL. 2001. Lactate efflux and the neuroenergetic basis of brain function. NMR Biomed 14:389–396.
Shulman RG, Hyder F, Rothman DL. 2009. Baseline brain energy supports the state of consciousness. Proc Natl Acad Sci U S A 106:11096–11101.
Shulman RG, Rothman DL. 1998. Interpreting functional imaging studies in terms of neurotransmitter cycling. Proc Natl Acad Sci U S A 95:11993–11998.
Shulman RG, Rothman DL, Hyder F. 1999. Stimulated changes in localized cerebral energy consumption under anesthesia. Proc Natl Acad Sci U S A 96:3245–3250.
Shulman RG, Rothman DL, Hyder F. 2007. A BOLD search for baseline. Neuroimage 36:277–281.
Smith AJ, Blumenfeld H, Behar KL, Rothman DL, Shulman RG, Hyder F. 2002. Cerebral energetics and spiking frequency: the neurophysiological basis of fMRI. Proc Natl Acad Sci U S A 99:10765–10770.
Tomasi D, Volkow ND. 2011. Association between Functional Connectivity Hubs and Brain Networks. Cereb Cortex 21:2003–2013.
Uludag K, Dubowitz DJ, Yoder EJ, Restom K, Liu TT, Buxton RB. 2004. Coupling of cerebral blood flow and oxygen consumption during physiological activation and deactivation measured with fMRI. Neuroimage 23:148–155.
van den Heuvel MP, Hulshoff Pol HE. 2010. Exploring the brain network: a review on resting-state fMRI functional connectivity. Eur Neuropsychopharmacol 20:519–534.
van Eijsden P, Hyder F, Rothman DL, Shulman RG. 2009. Neurophysiology of functional imaging. Neuroimage 45:1047–1054.
Vazquez AL, Masamoto K, Kim SG. 2008. Dynamics of oxygen delivery and consumption during evoked neural stimulation using a compartment model and CBF and tissue P_{O2} measurements. Neuroimage 42:49–59.
Wang K, van Meer MP, van der Marel K, van der Toorn A, Xu L, Liu Y, Viergever MA, Jiang T, Dijkhuizen RM. 2011. Temporal scaling properties and spatial synchronization of spontaneous blood oxygenation level-dependent (BOLD) signal fluctuations in rat sensorimotor network at different levels of isoflurane anesthesia. NMR Biomed 24:61–67.
Wei X, Yoo SS, Dickey CC, Zou KH, Guttmann CR, Panych LP. 2004. Functional MRI of auditory verbal working memory: long-term reproducibility analysis. Neuroimage 21:1000–1008.
Zhu XH, Du F, Zhang N, Zhang Y, Lei H, Zhang X, Qiao H, Ugurbil K, Chen W. 2009a. Advanced in vivo heteronuclear MRS Approaches for Studying Brain Bioenergetics Driven by Mitochondria. Methods Mol Biol 489:317–357.
Zhu XH, Zhang N, Zhang Y, Ugurbil K, Chen W. 2009b. New insights into central roles of cerebral oxygen metabolism in the resting and stimulus-evoked brain. J Cereb Blood Flow Metab 29:10–18.
Zhu XH, Zhang N, Zhang Y, Zhang X, Ugurbil K, Chen W. 2005. In vivo 17O NMR approaches for brain study at high field. NMR Biomed 18:83–103.

Address correspondence to:
D. S. Fahmeed Hyder
Magnetic Resonance Research Center (MRRC)
Yale University
N143 TAC
300 Cedar Street
New Haven, CT 06520

E-mail: fahmeed.hyder@yale.edu

(*Appendix follows* →)

Appendix: Estimation of Oxidative Energy Demand from Neural Activity

Behavior of neural populations is characterized by histograms of spiking rates of individual neurons (Maandag et al., 2007; Smith et al., 2002) when stimulated with the same stimulus, but from different baselines (Fig. 1A). Comparison of the histograms (composed of number of neurons firing at their respective signaling rates) for the two baseline states shows that in state X the fraction of population at lower frequencies makes a slightly greater contribution to the population's vote than in state Y (i.e., baseline state X < baseline state Y). However, the histograms for the two stimulated states have quite similar distributions (i.e., stimulated state X $\approx$ stimulated state Y), reached by redeployment (not recruitment) of a fraction of neuronal population. The same stimulated activities of the two baseline states agree well with magnitudes of changes in spiking rate and ΔCMR_{O2} during sensory stimulation (Fig. 1B, C).

Estimates of relative neuronal energy demanded in each baseline and stimulated state can be obtained by integrating each histogram using a linear relationship between oxidative energy demand (CMR_{O2}) and the number of cells (N_i) firing at a given rate (ν_i)

$$CMR_{O2} = G\sum N_i \nu_i \quad \text{(A1)},$$

where G in Eq. A1 is a scaling factor for pyramidal neurons (Maandag et al., 2007). For different brain states, relative neuronal energy calculated from experimentally measured histograms, as shown by Eq. A1, agrees quite well with oxidative energy demand measured by other techniques such as magnetic resonance spectroscopy and/or positron emission tomography (Hyder et al., 2001, 2006; Zhu et al., 2009a). However, careful considerations are necessary when histogram distributions span high and low frequencies in disproportionate fractions (Maandag et al., 2007).